

Calculation of hole subbands at the GaAs-Al_xGa_{1-x}As interface

U. Ekenberg and M. Altarelli

Max-Planck-Institut für Festkörperforschung, Hochfeld-Magnettabor,
166X, F-38042 Grenoble Cédex, France

(Received 21 May 1984)

The hole subbands in the inversion layer at the GaAs-Al_xGa_{1-x}As interface are calculated self-consistently in the Hartree approximation taking the degenerate structure of the valence band and the matching of the wave functions at the interface into account. The subbands versus the wave vector parallel to the interface are shown to be strongly nonparabolic and spin split. Only the highest subband pair has filled levels and about 64% of the charge is found to be in the uppermost of these spin subbands, in good agreement with experiment. The calculated effective masses are smaller than those found in cyclotron resonance experiments.

There has been much interest in the two-dimensional (2D) electron gas formed at the interface between GaAs and *n*-type Al_xGa_{1-x}As. The 2D hole gas at the interface to *p*-type Al_xGa_{1-x}As is more difficult to study experimentally, mainly because the mobility is lower for holes and the discontinuity in the valence band is smaller than in the conduction band. However, there have recently been some experimental studies of 2D hole gases,¹⁻⁴ which, because of the degenerate structure of the valence band, can be expected to exhibit some interesting features not found for electron subbands.

In calculations for inversion layers at the interface between Si and SiO₂ the wave function in Si was usually assumed to vanish at the interface; i.e., the SiO₂ barrier was assumed to be infinite.^{5,6} The discontinuity in the valence band between GaAs and Al_xGa_{1-x}As, which forms the bar-

rier for the holes in the inversion layer in GaAs, is only of the order 0.1 eV. Therefore, it is important to let the wave function penetrate into the Al_xGa_{1-x}As layer.

In this Rapid Communication we present calculations in the envelope function approximation for the hole subbands in the inversion layer at the ideal interface between a semi-infinite Al_{0.5}Ga_{0.5}As layer with an acceptor concentration $N_a = 10^{18} \text{ cm}^{-3}$ and a semi-infinite GaAs layer with an (unintentional) donor concentration $N_d = 10^{15} \text{ cm}^{-3}$.

A two-band Luttinger Hamiltonian^{7,8} is used in the spherical approximation ($\gamma_2 = \gamma_3 = \bar{\gamma}$).⁹ The conduction band and the split-off band are not taken explicitly into account. We choose the *z* direction as the quantization axis for angular momenta. For *k* in the (*xy*) plane the dispersion of the bands in the bulk are given by the eigenvalues of the block matrix¹⁰

$$\begin{pmatrix} E_v - (\gamma_1 + \bar{\gamma})k^2/2 & \sqrt{3}\bar{\gamma}(k_x - ik_y)^2/2 & 0 & 0 \\ \sqrt{3}\bar{\gamma}(k_x + ik_y)^2/2 & E_v - (\gamma_1 - \bar{\gamma})k^2/2 & 0 & 0 \\ 0 & 0 & E_v - (\gamma_1 + \bar{\gamma})k^2/2 & \sqrt{3}\bar{\gamma}(k_x + ik_y)^2/2 \\ 0 & 0 & \sqrt{3}\bar{\gamma}(k_x - ik_y)^2/2 & E_v - (\gamma_1 - \bar{\gamma})k^2/2 \end{pmatrix}. \quad (1)$$

To obtain the Hamiltonian matrix we choose the *x* direction to be perpendicular to the interface, replace k_x by $-i(d/dx)$, and add the self-consistent potential $V(x)$ along the diagonal. If we had inversion symmetry the upper and lower blocks would give the same energy bands (Kramers degeneracy). In the present case the inversion symmetry is broken by $V(x)$ and the two blocks give rise to two types of bands, split for $k \neq 0$, which we hereafter refer to as "spin subbands."

Each 2×2 block of the Hamiltonian is used with the appropriate valence-band parameters for the two materials and the matching of the wave functions at the interface is taken care of with use of a modified variational method including surface integrals and leading to wave functions which satisfy the appropriate boundary conditions.¹¹ This procedure has been described elsewhere.¹² The calculations are done for $T = 0 \text{ K}$. The valence-band parameters, the dielectric constants, and the distances between the Fermi level and the nearest band edge in the bulk are given in Table I for GaAs and Al_{0.5}Ga_{0.5}As.

For an Al content in Al_xGa_{1-x}As between 0.19 and 0.27, Dingle, Gossard, and Wiegmann¹⁶ found that 15% of the band-gap discontinuity ΔE_g is in the valence band. Similar values have also been obtained in theoretical calculations^{17,18} and other experiments.¹⁹ Baldereschi *et al.*¹⁷ also found that the whole band structure in Al_xGa_{1-x}As changes approximately linearly with *x*. For this reason we assume that the relation $\Delta E_v = 0.15\Delta E_g$ also holds for $x = 0.5$, although this has not yet been experimentally verified. For the variation of the Al_xGa_{1-x}As band gap with *x* we use the expression given by Dingle, Logan, and Arthur²⁰ and obtain $\Delta E_v = 94 \text{ meV}$. Since this parameter is uncertain we have also done calculations for $\Delta E_v = 86, 90, \text{ and } 100 \text{ meV}$.

The band diagram is shown in Fig. 1. The effect of the space charge of the ionized impurities is included in the depletion layer approximation. The depletion layer widths l_p and l_n are determined from the two constraints²¹

$$l_n N_d + N_s = l_p N_a \quad (2)$$

TABLE I. Parameters used in the calculations. Energy separation is between the Fermi level and nearest band edge [see Fig. 1(a)].

	Valence-band parameters		Dielectric constants	Energy separation (meV)
	γ_1	$\bar{\gamma}$		
GaAs	6.85 ^a	2.58 ^a	12.56 ($=\epsilon_1$) ^b	6 ($=\delta_1$) ^b
Al _{0.5} Ga _{0.5} As	5.15 ^a	1.813 ^a	11.06 ($=\epsilon_2$) ^c	35 ($=\delta_2$) ^d

^aReference 13. The γ 's for Al_{0.5}Ga_{0.5}As are taken as the average of $\gamma(\text{GaAs})$ and $\gamma(\text{AlAs})$. $\bar{\gamma} = (2\gamma_2 + 3\gamma_3)/5$.

^bReference 14.

^cAssuming that the variation with x at room temperature $\epsilon(\text{Al}_x\text{Ga}_{1-x}\text{As}) = \epsilon(\text{GaAs}) - 3.0x$ given in Ref. 15, p. 219, also holds at $T = 0$.

^dReference 1.

and

$$V_p(l_p) + V_n(-l_n) = E_g(\text{GaAs}) + \Delta E_v - \delta_1 - \delta_2, \quad (3)$$

where

$$V_n(-l_n) = \frac{2\pi}{\epsilon_1} N_d l_n^2 + V_{\text{inv}}(-\infty) \quad (4)$$

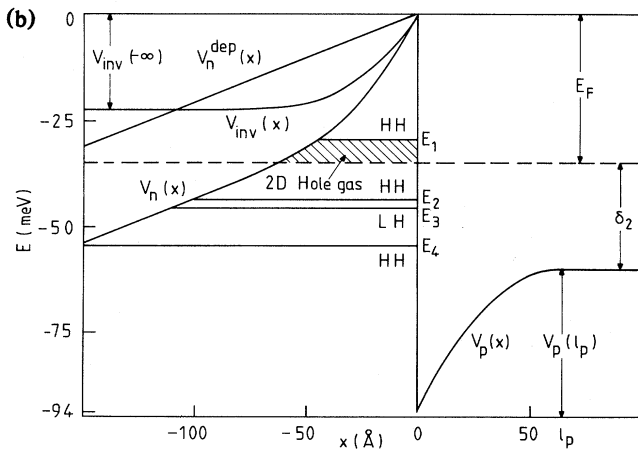
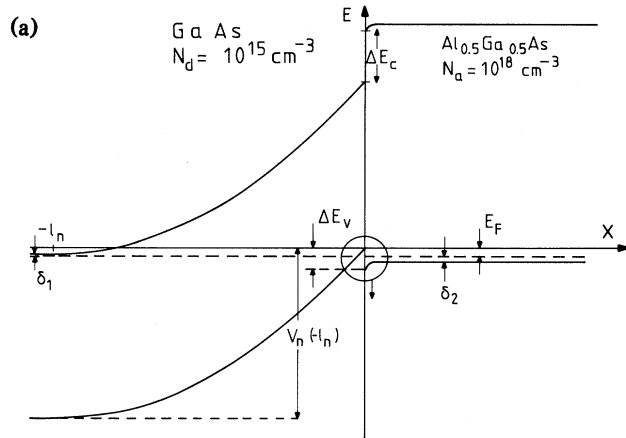


FIG. 1. Band diagram for the GaAs-Al_{0.5}Ga_{0.5}As interface. A portion of (a) is magnified in (b), where the energy levels at $k_y = 0$ and the potentials due to the inversion layer V_{inv} and to the depletion layers V_n^{dep} and V_p , and the total potential in GaAs $V_n = V_n^{\text{dep}} + V_{\text{inv}}$ are drawn.

and

$$V_p(l_p) = \frac{2\pi}{\epsilon_2} N_d l_p^2. \quad (5)$$

Here, $V_{\text{inv}}(x)$ is the Hartree potential due to the surface charge density N_s of the holes in the inversion layer. It is determined by solving Poisson's equation numerically to self-consistency. In the range of N_s of interest here, the Hartree approximation is rather crude, and many-body effects may be significant, as discussed by Ohkawa²² in the case of Si. However, his estimates, scaled down to the GaAs band parameters, show that the effect on the effective masses should not be too large.

In principle the Fermi level in the inversion layer relative to the GaAs valence-band edge could be determined from

$$E_F = \Delta E_v - V_p(l_p) - \delta_2. \quad (6)$$

However, the distance between the Fermi level and the valence band in Al_{0.5}Ga_{0.5}As, δ_2 , seems to be rather uncertain. The band bending $V_p(l_p)$ is also somewhat uncertain due to the use of the depletion layer approximation and it can also be influenced by surface defects. For these reasons we take the surface hole concentration N_s as an input parameter determined from experiment.

The difference in dielectric constant between GaAs and Al_{0.5}Ga_{0.5}As is small and, therefore, the image potential is neglected.

The envelope wave function is expanded in basis functions of two kinds:

$$\phi_i = N \exp[-b_i(z - a_i)^2] \quad (7)$$

and

$$\phi'_i = N'(z - a_i) \exp[-b_i(z - a_i)^2]. \quad (8)$$

The parameters a_i and b_i are chosen so that the absolute values of the subband energies are minimized. For six pairs (a_i, b_i) , i.e., 12 basis functions, the results are found to be quite insensitive to the choice of the parameters as long as they are reasonably chosen. We end up with 48×48 matrices to diagonalize for the two spin states and for each value of k_y , the wave vector parallel to the interface.

The subband energies as a function of k_y are displayed in Fig. 2 for a surface hole concentration $N_s = 5 \times 10^{11} \text{ cm}^{-2}$ (Ref. 23). Some important features are as follows: The subbands have a substantial splitting between the two spin states for $k_y \neq 0$. The second pair of subbands [from now on denoted by E_2 ; cf. Fig. 1(b)] bend up as k_y is increased

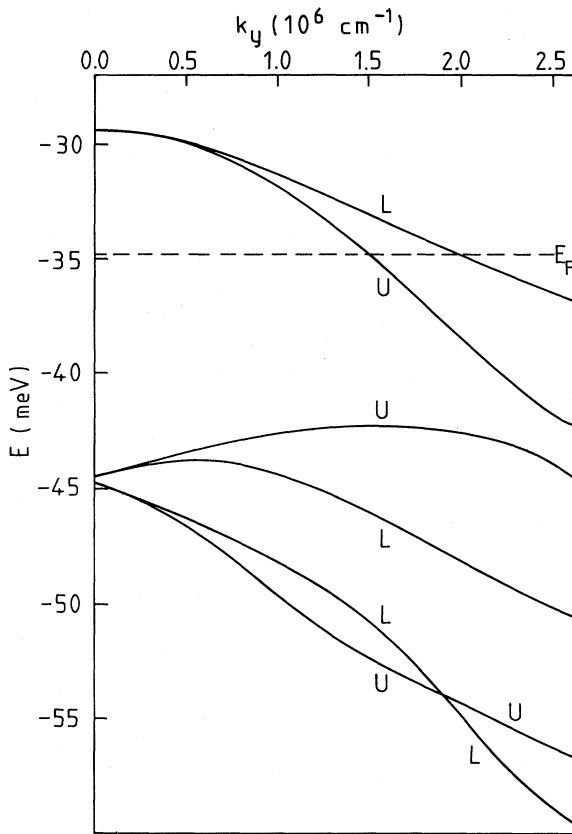


FIG. 2. Energy bands as a function of k_y for the GaAs- $\text{Al}_{0.5}\text{Ga}_{0.5}\text{As}$ interface for $\Delta E_v = 94$ meV. $N_s = 5 \times 10^{11} \text{ cm}^{-2}$, $N_a = 10^{18} \text{ cm}^{-3}$, and $N_d = 10^{15} \text{ cm}^{-3}$. The letters U and L denote the bands obtained from upper and lower blocks, respectively, of the matrix in Eq. (1).

from zero; i.e., they have electronlike masses. E_2 is very close to E_3 at $k_y = 0$, differing by only 0.2 meV. The spin states for E_2 and E_3 cross each other at $k_y = 5.5 \times 10^6 \text{ cm}^{-1}$ (not shown) and at $k_y = 1.9 \times 10^6 \text{ cm}^{-1}$, respectively. We find the Fermi level to be 5.4 meV below E_1 . Only the uppermost pair of spin subbands (E_1) are populated by holes. The Fermi wave vectors for these subbands are 1.5×10^6 and $2.0 \times 10^6 \text{ cm}^{-1}$, respectively. Approximately 64% of the charge is in the uppermost spin subband.

An analysis of the eigenfunctions indicates that E_1 and E_2 are heavy-hole bands at $k_y = 0$ while E_3 is a light-hole band at $k_y = 0$. When $k_y \neq 0$, the bands have mixed heavy- and light-hole character, and for E_2 and E_3 , the mixing is pronounced even for quite small k_y values.

The cyclotron effective masses are calculated using the classical expression

$$m^* = \frac{1}{2\pi} \frac{dA(E)}{dE} \Big|_{E=E_F}, \quad (9)$$

where $A(E)$ is the area in k space of the surface with constant $E(k)$. We find $m^* = 0.44$ for the uppermost spin band and $m^* = 0.17$ for the band which is degenerate with this band at $k_y = 0$. The potentials in GaAs and in $\text{Al}_{0.5}\text{Ga}_{0.5}\text{As}$ are shown in Fig. 1(b).

We have investigated the effect of the barrier height on

the hole subbands also for other values of ΔE_v , and found that each band is essentially rigidly shifted as the barrier height is changed. However, it is found that the light-hole-like bands are shifted considerably more than the heavy-hole-like bands. For $\Delta E_v = 86$ meV the heavy- and light-hole-like bands are shifted upwards by about 0.5 and 1 meV, respectively, compared to Fig. 2 ($\Delta E_v = 94$ meV). The second and third subbands (E_2' and E_3') have almost the same k_y dispersion up to $k_y \approx 2 \times 10^6 \text{ cm}^{-1}$ as E_2 and E_3 in Fig. 2, but for $\Delta E_v = 86$ meV E_2' is a light-hole band and is about 0.3 meV above the heavy-hole band E_3' . These two bands coincide at $k_y = 0$ for $\Delta E_v \approx 90$ meV.

This behavior is qualitatively different from that of electron subbands in GaAs. We have done some calculations for triangular wells with different barrier heights for a non-degenerate band (like the conduction band) and compared with the analytical solution for the infinite well.²⁴ It is found that the lowest subbands are almost exactly shifted by the same amount as the barrier height is changed if it is much larger than the energy levels. Even if the band energies differ several meV from the results for the infinite triangular well the interband separations change by less than 0.1 meV. A similar conclusion was drawn by Stern²⁵ for n -channel Si inversion layers.

Next we want to compare our results with other experimental and theoretical results. Störmer *et al.*³ have observed the quantized Hall effect for holes in a sample with the same N_a and N_s as in the present calculation and determined the effective masses and the population of the individual spin subbands.²⁶ Their cyclotron resonance results for the effective masses were 0.60 and 0.38. Shubnikov-de Haas experiments^{1,3} gave a mass close to the second value. Especially the lower effective mass is considerably higher than that found in the present calculation. They also found that 61% of the holes were in the upper spin subband, in good agreement with our result.

Their sample differed from the structure considered in this calculation in that it had an undoped $\text{Al}_{0.5}\text{Ga}_{0.5}\text{As}$ spacer layer of thickness $d = 70 \text{ \AA}$ between the GaAs layer and the doped $\text{Al}_{0.5}\text{Ga}_{0.5}\text{As}$ layer. The effect of a spacer layer can, in principle, be taken into account in the present calculation by replacing Eq. (5) with

$$V_p(l_p) = \frac{2\pi}{\epsilon_2} N_a l_p^2 + \frac{4\pi}{\epsilon_2} N_a l_p d. \quad (10)$$

We then find that $V_p(l_p)$ becomes about 110 meV, i.e., larger than ΔE_v . Thus, it appears that there should be no 2D hole gas at the interface. However, one must consider the finite width (500 \AA) of the doped $\text{Al}_{0.5}\text{Ga}_{0.5}\text{As}$ layer. At the other side of this layer one should expect some band bending of a magnitude which depends on the details there. The observation of the quantized Hall effect in this sample indicates that it has no parallel conduction²⁷ and if we assume that impurity conduction is possible for $N_a = 10^{18} \text{ cm}^{-3}$ we can conclude that the doped layer is, in fact, depleted and that the band diagram obtained from Eqs. (2)–(4) and (10) is no longer relevant.

One important effect to consider is that the cyclotron resonance experiments were carried out in fairly strong magnetic fields while the present calculation is for zero magnetic field. Recent theoretical²⁸ and experimental²⁹ results for the single GaAs well indicate that the effective masses for holes can be strongly influenced by the magnetic field. A calcula-

tion of the Landau levels in the presence of a magnetic field will be reported later. Furthermore, many-body corrections to the effective mass can be important. It should also be noted that the width of the GaAs layer in Ref. 3 was about 10000 Å while the depletion layer width l_n in this calculation is found to be 14500 Å.

The only other calculation known to us for this system has recently been presented.³⁰ This calculation differed from ours in two respects: The wave function was taken to be zero at the interface, but on the other hand, the spherical approximation was not made. The cyclotron effective masses 0.61 and 0.15 were obtained, in fair agreement with our results. The agreement with experiment for the higher mass is good, but the discrepancy for the lower one is increased.

In conclusion, we have calculated the hole subbands of an inversion layer at a semiconductor heterostructure interface.

Interesting features like subbands bending upwards near $k_y=0$ and spin splitting of the subbands are seen. Experiments in magnetic fields^{1,3} have given effective masses larger than the ones calculated in this Rapid Communication. Experimental results for transitions between hole subbands without a magnetic field would be desirable for a quantitative comparison with the present calculation.

We are indebted to Dr. J. C. Maan for numerous valuable discussions. We are also grateful to Dr. A. Fasolino, Dr. E. Molinari, Dr. J. Chroboczek, Dr. C. Uihlein, and Dr. K. Heime for illuminating discussions concerning various aspects of this work. One of us (U.E.) gratefully acknowledges the financial support from the Deutscher Akademischer Austauschdienst. The numerical results were obtained with the computer facilities of the Centre de Calcul Vectoriel pour la Recherche, Palaiseau.

-
- ¹H. L. Störmer and W.-T. Tsang, *Appl. Phys. Lett.* **36**, 685 (1980).
²H. L. Störmer, A. Chang, D. C. Tsui, J. C. M. Hwang, A. C. Gossard, and W. Wiegmann, *Phys. Rev. Lett.* **50**, 1953 (1983).
³H. L. Störmer, Z. Schlesinger, A. Chang, D. C. Tsui, A. C. Gossard, and W. Wiegmann, *Phys. Rev. Lett.* **51**, 126 (1983).
⁴H. L. Störmer, A. C. Gossard, W. Wiegmann, R. Blondel, and K. Baldwin, *Appl. Phys. Lett.* **44**, 139 (1984).
⁵E. Bangert, K. v. Klitzing, and G. Landwehr, in the *Proceedings of the 12th International Conference on the Physics of Semiconductors*, edited by M. Pilkuhn (Teubner, Stuttgart, 1974), p. 714.
⁶F. J. Ohkawa and Y. Uemura, *Suppl. Prog. Theor. Phys.* **57**, 164 (1975).
⁷J. M. Luttinger and W. Kohn, *Phys. Rev.* **97**, 869 (1955).
⁸J. M. Luttinger, *Phys. Rev.* **102**, 1030 (1956).
⁹A. Baldereschi and N. O. Lipari, *Phys. Rev. B* **8**, 2697 (1973).
¹⁰Atomic units ($\hbar = m_0 = e^2 = 1$) are used throughout the paper.
¹¹H. Schlosser and P. M. Marcus, *Phys. Rev.* **131**, 2529 (1963), especially Appendix I.
¹²M. Altarelli, *Phys. Rev. B* **28**, 842 (1983).
¹³*Semiconductors*, edited by O. Madelung, M. Schulz, and H. Weiss, Landolt-Börnstein Numerical Data and Functional Relationships in Science and Technology, Group III, Vol. 17 (Springer, Berlin, 1982).
¹⁴G. E. Stillman, D. M. Larsen, C. M. Wolfe, and R. C. Brandt, *Solid State Commun.* **9**, 2245 (1971).
¹⁵H. C. Casey, Jr. and M. B. Panish, *Heterostructure Laser, Part A. Fundamental Principles* (Academic, New York, 1978).
¹⁶R. Dingle, A. C. Gossard, and W. Wiegmann, *Phys. Rev. Lett.* **34**, 1327 (1975).
¹⁷A. Baldereschi, E. Hess, K. Maschke, H. Neumann, K.-R. Schulze, and K. Unger, *J. Phys. C* **10**, 4709 (1977).
¹⁸J. Sánchez-Dehesa and C. Tejedor, *Phys. Rev. B* **26**, 5824 (1982).
¹⁹R. People, K. W. Wecht, K. Alavi, and A. Y. Cho, *Appl. Phys. Lett.* **43**, 118 (1983).
²⁰R. Dingle, R. A. Logan, and J. R. Arthur, in Ref. 15, p. 193.
²¹Cf. T. C. Hsieh, K. Hess, J. J. Coleman, and P. D. Dapkus, *Solid State Electron.* **26**, 1173 (1983).
²²F. J. Ohkawa, *J. Phys. Soc. Jpn.* **41**, 122 (1976).
²³Calculations for other values of N_s , N_a , N_d , and ΔE_v will be presented in a forthcoming publication.
²⁴L. D. Landau and E. M. Lifshitz, *Quantum Mechanics: Non-relativistic Theory* (Addison-Wesley, Reading, 1958), p. 70.
²⁵F. Stern, *Solid State Commun.* **21**, 163 (1977).
²⁶The other quantities given in Ref. 3 are derived from the effective masses and subband populations.
²⁷E. F. Schubert, K. Ploog, H. Dämbkes, and K. Heime, *Appl. Phys. A* **33**, 63 (1984).
²⁸A. Fasolino and M. Altarelli, in *Two-Dimensional Systems, Heterostructures and Superlattices*, edited by G. Bauer, F. Kuchar, and H. Heinrich, (Springer, Berlin, 1984), p. 176.
²⁹J. C. Maan (private communication).
³⁰G. Landwehr and E. Bangert, in *Two-Dimensional Systems, Heterostructures and Superlattices*, edited by G. Bauer, F. Kuchar, and H. Heinrich (Springer, Berlin, 1984), p. 40.